Langmuir

Article

pubs.acs.org/Langmuir

Preparation of Highly Anisotropic Cobalt Ferrite/Silica Microellipsoids Using an External Magnetic Field

Sébastien Abramson,*[,†] Vincent Dupuis,[†] Sophie Neveu,[†] Patricia Beaunier,[‡] and David Montero[§]

[†]Laboratoire de Physicochimie des Electrolytes, et Nanosystèmes Interfaciaux, PHENIX (UMR 8234 UPMC-CNRS), [‡]Laboratoire de Réactivité de Surface, LRS (UMR 7197 UPMC-CNRS), and [§]Institut des Matériaux de Paris Centre, IMPC (FR 2482), Université Pierre et Marie Curie, 4, place Jussieu, 75 252 Paris Cedex 05, France

Supporting Information

ABSTRACT: Magnetic cobalt ferrite/silica microparticles having both an original morphology and an anisotropic nanostructure are synthesized through the use of an external magnetic field and nanoparticles characterized by a high magnetic anisotropy. The association of these two factors implies that the ESE (emulsion and solvent evaporation) sol–gel method employed here allows the preparation of silica microellipsoids containing magnetic nanoparticles aggregated in large chains. It is clearly shown that without this combination, microspheres characterized by an isotropic distribution of the magnetic nanoparticles are obtained. While the chaining of the cobalt ferrite nanoparticles inside the silica matrix is related to the increase of their magnetic dipolar interactions, the ellipsoidal shape of the microparticles may be explained by the elongation of the sol droplets in the direction of the external magnetic field during the synthesis. Because of their highly anisotropic structure, these microparticles exhibit permanent magnetic moments, which are responsible, at a larger scale, for the existence of strong magnetic dipolar interactions. Therefore, when they are dispersed in water, the microellipsoids self-assemble into large and irregular chains. These interactions can be reinforced by the use of external magnetic field, allowing the preparation of very large permanent chains. This research illustrates how nanostructured particles exhibiting complex architectures can be elaborated through simple, fast, and low-cost methods, such as the use of external fields in combination with soft chemistry.

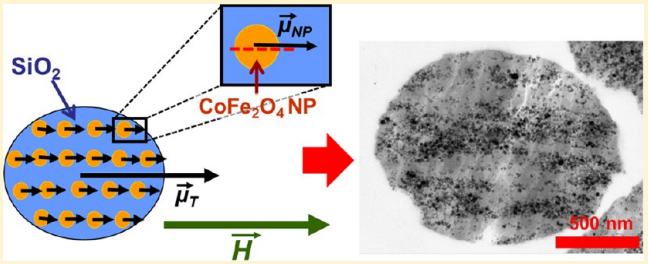

Colloidal particles have long been an important subject of investigation for many researchers in various fields, due to their applications in various industrial domains, and to their interest for the understanding of several physicochemical concepts. The first efforts were focused on the synthesis and study of monodisperse colloids of various sizes (from nanometer to micrometer), generally having some spherical shapes and composed of a single phase.[1−4] Now, the challenge is to obtain particles with original shapes and complex structures that can show unexpected physicochemical properties, opening new fields of applications for these materials.[4−7] This is well-illustrated in the case of the magnetic nanocomposite particles. These materials are generally composed of magnetic nanoparticles such as cobalt, nickel, iron, ferrite, maghemite, or magnetite encapsulated in an inorganic, organic, or hybrid matrix.[8−12] They combine the magnetic properties provided by the nanoparticles with additional characteristics such as a high chemical, biological, or thermal stability, optical transparency, high porosity, or capacity of adsorption or encapsulation. Consequently, they have been widely studied as catalysts, adsorbents for water treatment or for analysis of biomolecules, MRI contrast or magnetic hyperthermia agents, drug delivery matrixes, biological or environmental sensors, and magneto-optical devices.[8−13] Frequently, these materials are characterized by a spherical shape with a mean diameter varying from few nanometers to several micrometers, and by an isotropic dispersion of the magnetic nanoparticles in the nonmagnetic matrix.[8−12] However, there has been an increasing interest in the preparation of magnetic nanocomposite particles with more complex shapes and/or nanostructures.[8,10,12,13] In particular, these complex architectures lead to enhanced or different magnetic properties in comparison to their reference counterpart. For example, it has been recently shown that polyhedron-shaped magnetic nanocomposite particles having specific surface facets exhibited ferromagnetic properties, although they were composed of an antiferromagnetic material.[14] Among the various strategies used for the preparation of these unusual architectures, an elegant method consists of using an external magnetic field capable of increasing the dipolar interactions between the magnetic nanoparticles, to induce their self-assembly into chain-like structures. This has been exploited by several authors to prepare highly anisotropic nanocomposite particles such as wires,[15−18] rigid chains,[19−23] fibers,[24,25] rods,[26,27] flagella-like particles,[28] or opaline beads,[29,30] and at larger scale, anisotropic films,[31,32] or monoliths.[33,34] In some recent works, a slightly different procedure was also developed, where the anisotropy of

Received: April 22, 2014
Revised: July 10, 2014
Published: July 16, 2014

   dx.doi.org/10.1021/la501547q | *Langmuir* 2014, 30, 9190−9200

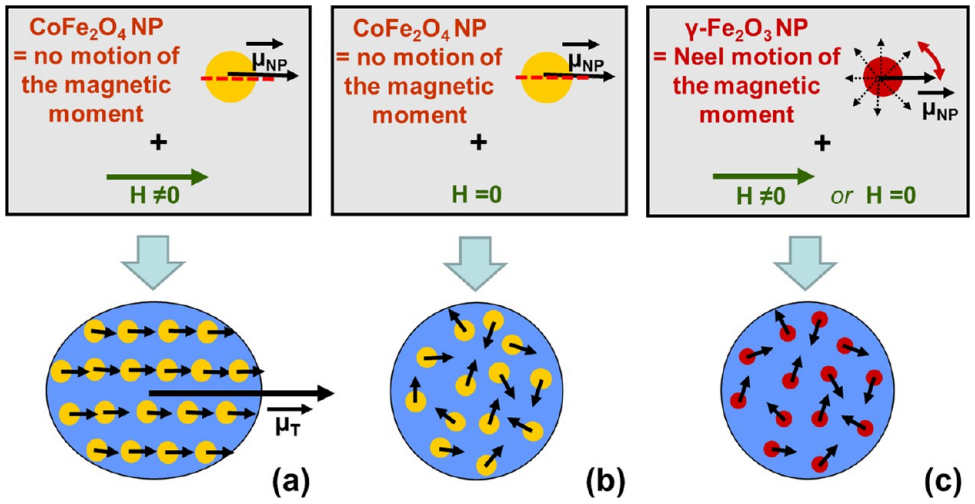

Figure 1. Theoretical structures of the synthesized samples. (a) Microellipsoids synthesized with $CoFe_2O_4$ nanoparticles having a high value of E_a, in the presence of external magnetic field (H-$CoFe_2O_4/SiO_2$ sample). (b) Reference sample synthesized with $CoFe_2O_4$ nanoparticles having a high value of E_a in the absence of external magnetic field ($CoFe_2O_4/SiO_2$ sample). (c) Reference samples synthesized with γ-Fe_2O_3 nanoparticles having a low value of E_a in the presence or in the absence of external magnetic field (γ-Fe_2O_3/SiO_2 and H-γ-Fe_2O_3/SiO_2 samples). Insets: (a and b) At ambient temperature, the magnetic moment of the $CoFe_2O_4$ nanoparticle is blocked in the direction of the easy axis. (c) At ambient temperature, the magnetic moment of the γ-Fe_2O_3 nanoparticle is free to rotate.

magnetic nanocomposite particles[35] or films[36] was induced through the external force resulting from the magnetic field gradient. These oriented structures often have an impact on the magnetic, optical, and colloidal properties of these materials, which consequently exhibit fascinating features, such as the possibility, when an external magnetic field is applied, to diffract the visible light,[29,30] to self-organize into zigzag chains,[25] to rotate around their center of gravity,[23,26,35] or to "swing" in a liquid medium.[28]

Here, we report the synthesis and characterization of magnetic silica nanocomposite particles having both a micro-sized ellipsoidal shape and a highly anisotropic internal structure. These microellipsoids are constituted by magnetic nanoparticles anisotropically self-assembled in a silica matrix. Because of this unique structure, they present some strong individual magnetic moments, which allow them, when suspended in water, to self-assemble into chains at a larger scale, even in the absence of an external magnetic field.

To prepare these materials, we used a strategy that can be summed into two key points. First, inorganic magnetic nanoparticles characterized by strong magnetic anisotropy energy have been used as starting materials. Anisotropy energy is an important parameter in magnetic materials.[37] For an isolated nanoparticle having a single ferro- or ferrimagnetic domain, the anisotropy energy barrier, E_a, can be obtained by the following equation (in the absence of applied magnetic field):

$$E_a = KV \quad (1)$$

where K is the magnetic anisotropy constant, and V is the volume of the nanoparticle.

The constant K generally depends on the crystalline anisotropy, the shape, and the surface of the nanoparticle. "Hard" ferro- or ferrimagnetic phases such as cobalt ferrite ($CoFe_2O_4$), iron (Fe), or platinum−iron (FePt) are characterized by a high value of K, to the contrary of "soft" ferrimagnetic phases such as magnetite (Fe_3O_4) or maghemite (γ-Fe_2O_3). Moreover, because eq 1 shows that E_a depends on V, larger nanoparticles are generally characterized by a higher value of E_a. At ambient temperature, the magnetic moment (μ) of a hard nanoparticle (i.e., having a high value of E_a) is blocked along the easy axis of the nanoparticle, because the value of the thermal energy kT is not sufficient to allow fast thermal fluctuations of μ (Neel motion). This leads to the existence of strong magnetic dipolar interactions between the nanoparticles, even in the absence of an external magnetic field, which are able in some case to induce their directional self-assembly.[38−41]

The second key point of this work consists of using an external magnetic field (H) during the synthesis, to create a directional orientation of the nanoparticles, which tend to align their easy axis parallel to the direction of H. This will result first in a strong increase of the dipolar interactions between the magnetic nanoparticles inside the silica microparticles. Moreover, each microparticle will be characterized by a strong permanent magnetic moment (μ_T), resulting from the addition of the blocked and oriented individual magnetic moments of the encapsulated magnetic nanoparticles (see Figure 1a).

While the previous works on the magnetic field-induced self-assembly of nanoparticles have been limited to the preparation of highly elongated structures constituted by one or several chains of permanently linked nanoparticles,[15−28] or to the encapsulation of these chains in continuous polymeric matrixes such as large spherical beads (more than 20 μm in size),[29,30] films,[31,32] or monoliths,[33,34] herein the chained nanoparticles are encapsulated for the first time in small silica microellipsoids (less than 10 μm in size). In addition, a more complex effect of the magnetic field is evidenced here. Thus, we report a multiscale effect of the magnetic field, because its use, in combination with hard magnetic nanoparticles, allows a control of the anisotropy of the microparticles on three levels, that is, their internal structure at the nanometer scale, their shape at the micrometer scale, and their aggregation properties at larger scale.

RESULTS AND DISCUSSION

Preparation and Characterization of the Microellipsoids. To prepare the magnetic nanocomposite microellipsoids, it was necessary to use an acidic dispersion of

dx.doi.org/10.1021/la501547q | Langmuir 2014, 30, 9190−9200

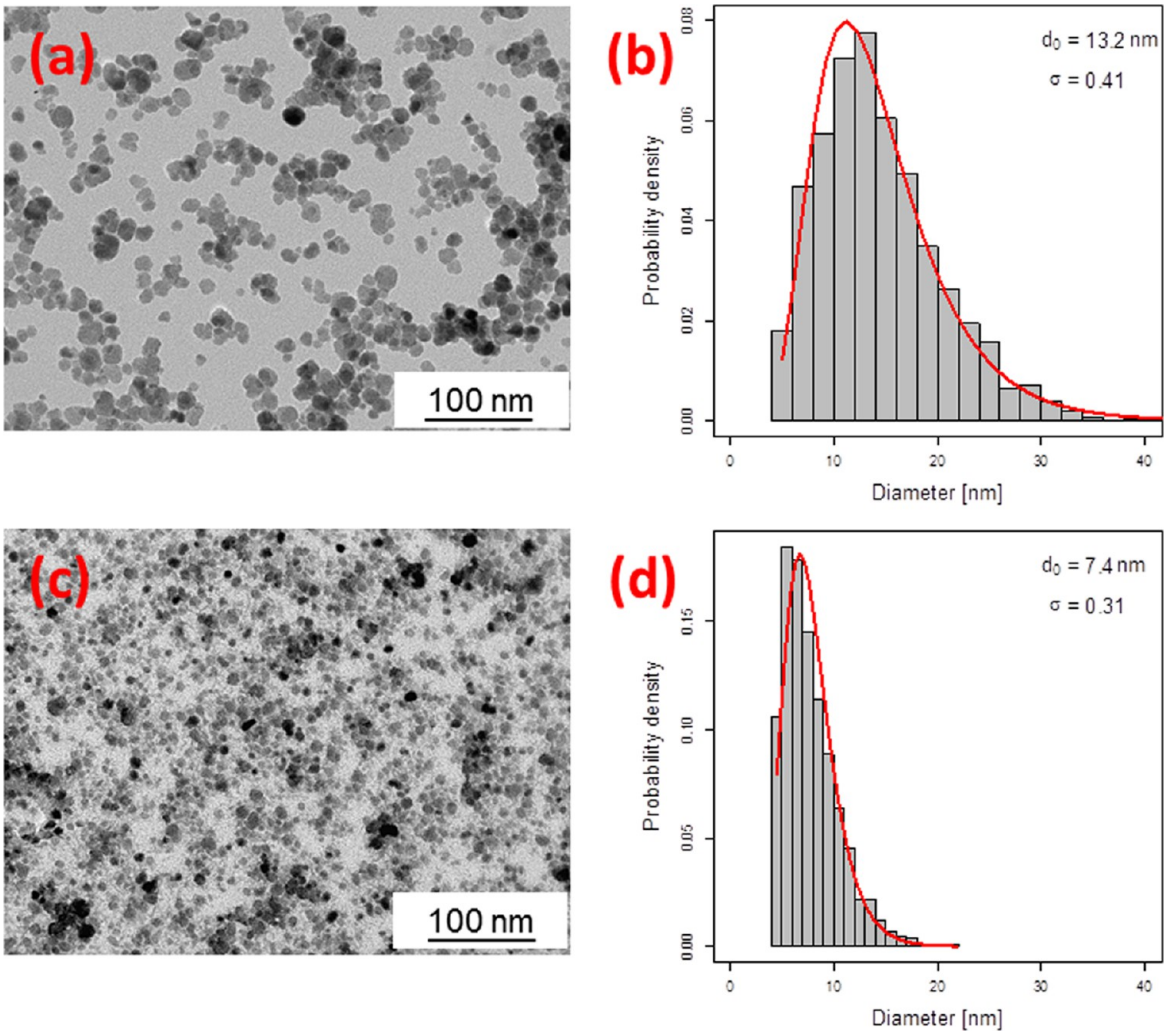

Figure 2. TEM images of the precursor nanoparticles and their resulting size distributions. (a) TEM image of the $CoFe_2O_4$ nanoparticles. (b) Experimental (gray histogram) and theoretical log-normal (red curve) size distributions of the $CoFe_2O_4$ nanoparticles. (c) TEM image of the γ-Fe_2O_3 nanoparticles. (d) Experimental (gray histogram) and theoretical log-normal (red curve) size distributions of the γ-Fe_2O_3 nanoparticles.

magnetic cobalt ferrite ($CoFe_2O_4$) nanoparticles as starting material. These nanoparticles were synthesized by the coprecipitation of Co^{2+} and Fe^{3+} ions followed by a hydrothermal treatment, according to a previously published method.[42] This procedure allows the preparation of nanoparticles characterized by a relatively large mean diameter (d_0 = 13.2 nm) with a polydispersity index of σ = 0.4. The TEM image and the resulting size distributions of the $CoFe_2O_4$ precursor are given in Figure 2. These nanoparticles were chosen because of their high value of E_a. Indeed, $CoFe_2O_4$ is a crystalline phase with a relatively high anisotropy constant ($K \approx$ 200 kJ m^{-3}). Using eq 1, a theoretical value for E_a was calculated, corresponding to 58 kT (T = 298 K, and k is the Boltzmann constant), which means that these nanonoparticles have a blocked magnetic moment at ambient temperature (Figure 1a,b). More details about the characteristics of the $CoFe_2O_4$ nanoparticles can be found in the Supporting Information (Figure S1).

The magnetic microellipsoids (also called H-$CoFe_2O_4$/SiO_2 sample) were prepared via a modified ESE (emulsion solvent evaporation) procedure[43] described in our previous publication.[44] In brief, a magnetic sol was first prepared using an acidic dispersion of the $CoFe_2O_4$ nanoparticles and a silica precursor (TEOS) previously hydrolyzed in an acidic solution. This sol was added to a vegetable oil containing a small amount of Arlacel P135, a hydrophobic surfactant. The obtained water-in-oil emulsion was evaporated under vacuum, to decrease the gel time of the silica in the sol droplets. Hence, the emulsion was mechanically stirred all night, in the presence of a permanent magnetic field of 1500 Oe, obtained by the use of two cuboid ferrite magnets in parallel. A photograph of the experimental setup can be found in the Supporting Information (Figure S2). Finally, the emulsion was broken by addition of acetone, and the particles were thoroughly washed with acetone before being dried at 70 °C. For comparison, three reference samples were prepared by the same method. The first sample was prepared using the same batch of $CoFe_2O_4$ nanoparticles in the absence of the external magnetic field ($CoFe_2O_4$/SiO_2 sample). The two other samples were prepared using a dispersion of γ-Fe_2O_3 magnetic nanoparticles having a low value of E_a (K = 35 kJ m^{-3}, d_0 = 7.4 nm, and $E_a \approx 2kT$ at T = 298 K, see Figure 2 for their TEM image and size distributions), respectively, in the absence and in the presence of the external magnetic field (γ-Fe_2O_3/SiO_2 and H-γ-Fe_2O_3/SiO_2 samples). The γ-Fe_2O_3 nanoparticles are thus characterized by a fast Neel motion of their magnetic moment at ambient temperature (Figure 1, inset (c)). The

dx.doi.org/10.1021/la501547q | Langmuir 2014, 30, 9190−9200

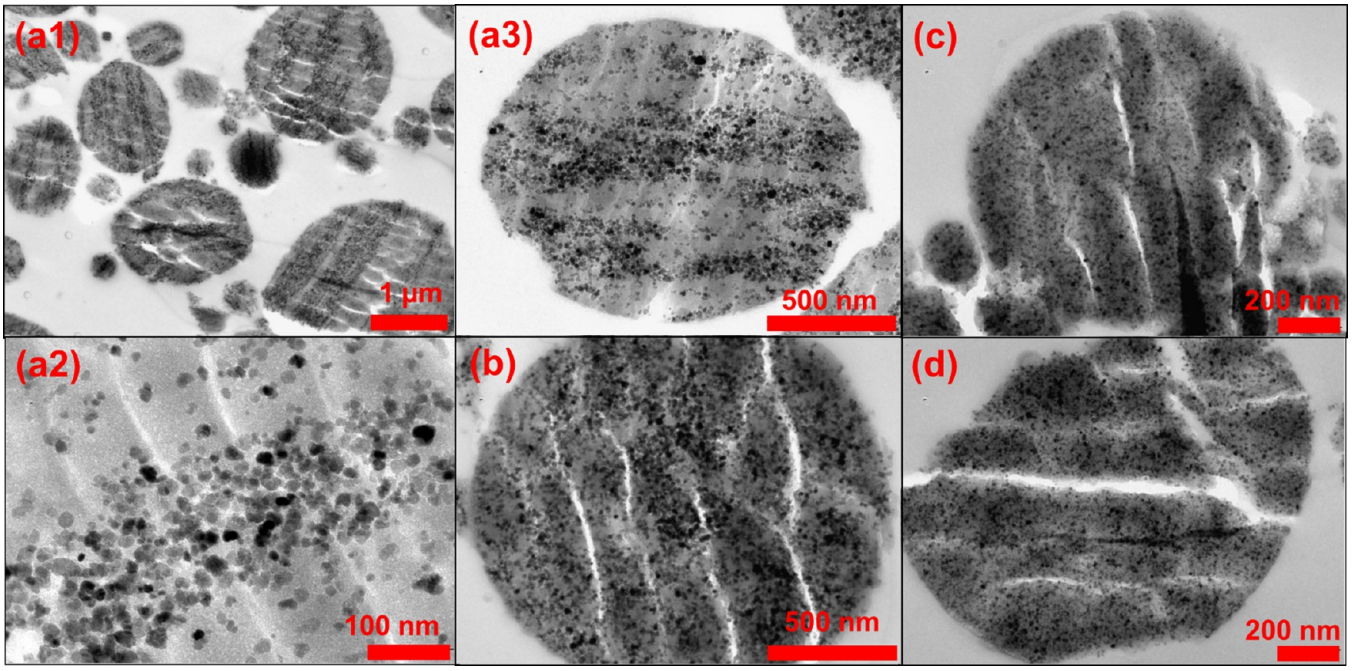

Figure 3. TEM images of the microparticles. (a1)−(a3) H-$CoFe_2O_4/SiO_2$ microellipsoids at low (a1), high (a2), and medium magnifications (a3). (b) $CoFe_2O_4/SiO_2$ reference sample, medium magnification. (c) γ-Fe_2O_3/SiO_2 reference sample, medium magnification. (d) H-γ-Fe_2O_3/SiO_2 reference sample, medium magnification.

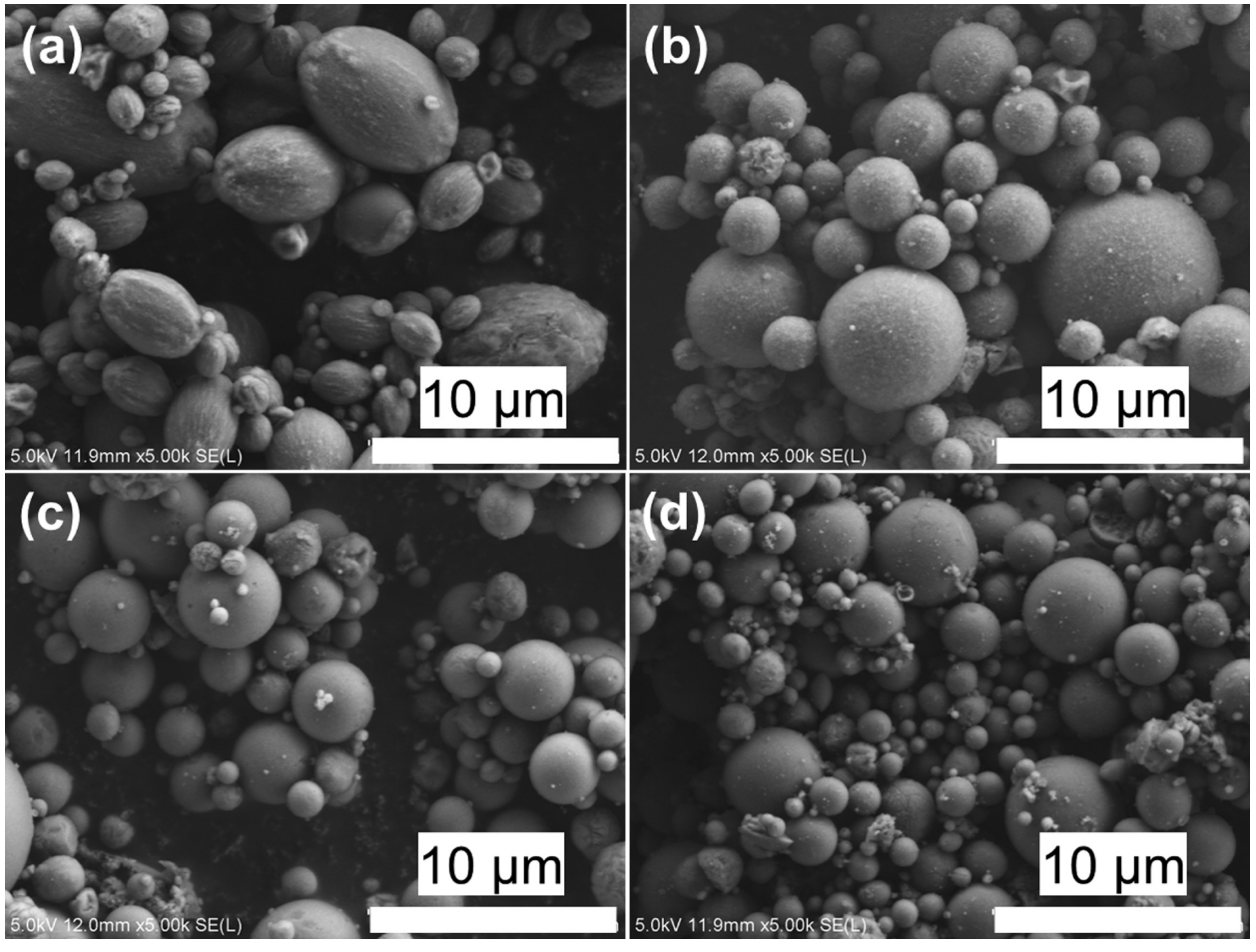

Figure 4. SEM images of the microparticles. (a) H-$CoFe_2O_4/SiO_2$ microellipsoids. (b) $CoFe_2O_4/SiO_2$ reference sample. (c) γ-Fe_2O_3/SiO_2 sample. (d) H-γ-Fe_2O_3/SiO_2 reference sample.

dx.doi.org/10.1021/la501547q | *Langmuir* 2014, 30, 9190−9200

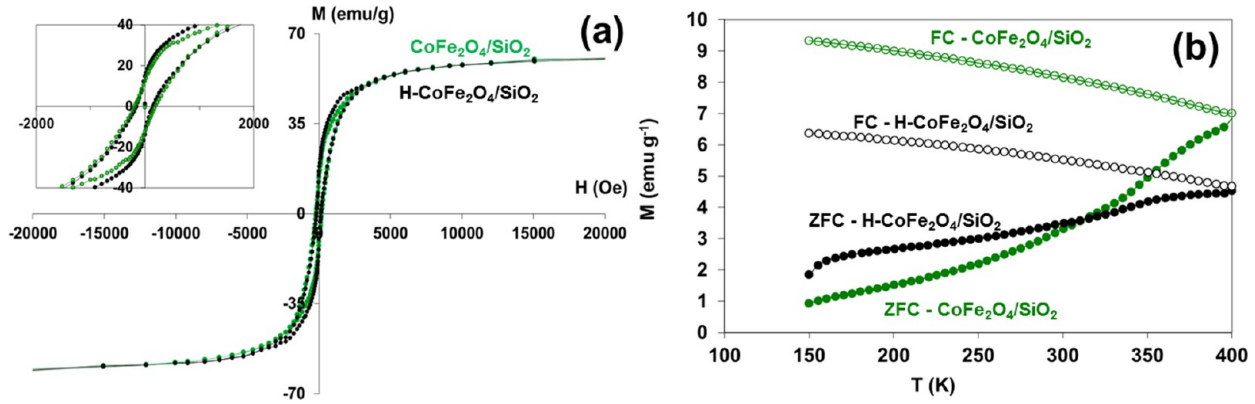

Figure 5. (a) Magnetization−demagnetization curves of the H-$CoFe_2O_4/SiO_2$ microellipsoids (black dots) and $CoFe_2O_4/SiO_2$ reference sample (green dots). Inset: Magnification of the low-field part of the curves. (b) ZFC/FC curves (magnetization versus temperature) of the H-$CoFe_2O_4/SiO_2$ microellipsoids (●, ZFC curve; ○, FC curve) and $CoFe_2O_4/SiO_2$ sample (green ●, ZFC curve; green ○, FC curve). All of the values of magnetization are normalized to 1 g of $CoFe_2O_4$.

Table 1. Magnetic Properties of the H-$CoFe_2O_4/SiO_2$ Microellipsoids, and $CoFe_2O_4/SiO_2$, γ-Fe_2O_3/SiO_2, H-γ-Fe_2O_3/SiO_2 Reference Samples

sample	m_s (emu g^{-1})[a]	w_{NP} (% w/w)[b]	M_0 (emu g^{-1})[c]	M_R (emu g^{-1})[c]	H_C (Oe)	T_b (K)
H-$CoFe_2O_4/SiO_2$	20.9	33.7	1.1	14.5	150	>400
$CoFe_2O_4/SiO_2$	21.3	34.3	0	12.4	190	>400
γ-Fe_2O_3/SiO_2	18.1	33.5	0	1.2	10	80
H-γ-Fe_2O_3/SiO_2	18.3	33.9	0	1.2	10	85

[a]The saturation magnetization m_s is given in emu/g of composite sample. [b]The weight fractions in magnetic nanoparticles, w_{NP}, were obtained by $w_{NP} = m_s/M_s$, where M_s is the saturation magnetization of the magnetic nanoparticles. [c]M_0 and M_R are given in emu/g of magnetic nanoparticles (normalized values).

theoretical structures of the synthesized samples are presented in Figure 1.

Figure 3 shows the TEM images of the microellipsoids and blank samples at various magnifications. In the H-$CoFe_2O_4/SiO_2$ sample, the magnetic nanoparticles are strongly aggregated, forming some long and large chains (Figure 3a1−a3). This spectacular phenomenon is observed in all of the microparticles, although the length and width of the chains are not regular. The shape of the microparticles seems to be ellipsoidal, and all of the chains are oriented along the main axis of the ellipsoids. At high magnification (Figure 3a2 and a3), we observe the coexistence of large chains where the $CoFe_2O_4$ nanoparticles are both laterally and longitudinally aggregated, with single linear chains composed of few $CoFe_2O_4$ nanoparticles. It is also suggested from the higher magnification image (Figure 3a3) that the $CoFe_2O_4$ cores are surrounded by silica, indicating the absence of demixing between the two phases. On the contrary, the magnetic nanoparticles in the three reference samples are poorly aggregated and their distribution is isotropic (Figure 3b−d). For the $CoFe_2O_4/SiO_2$ sample, the nanoparticles seem to be slightly aggregated (Figure 3b), whereas the γ-Fe_2O_3 nanoparticles are homogeneously distributed without any aggregation, independently of the presence of an external magnetic field during the synthesis (Figure 3c and d). The chaining of the nanoparticles in the H-$CoFe_2O_4/SiO_2$ sample is therefore attributed to a synergistic effect of the magnetic field and the use of the $CoFe_2O_4$ nanoparticles. The magnetic field considerably reinforces the longitudinal and lateral magnetic dipolar interactions between the nanoparticles and orients them in the direction of the external magnetic field.[38] In the $CoFe_2O_4/SiO_2$ sample, the slight and nondirectional aggregation of the nanoparticles may be explained by the presence of moderate magnetic dipolar interactions between the nanoparticles existing at zero field. In the γ-Fe_2O_3/SiO_2 and H-γ-Fe_2O_3/SiO_2 samples, no aggregation occurs, even in the presence of the external magnetic field, because the magnetic dipolar interactions between the γ-Fe_2O_3 nanoparticles are considerably weakened by their lower energy anisotropy.

The ellipsoidal morphology of the H-$CoFe_2O_4/SiO_2$ particles was confirmed by SEM (Figure 4a). The microellipsoids are polydisperse, and by counting the size of 500 particles on the SEM images, we determined that they have a mean Ferret diameter of 2.2 μm (standard deviation = 1.9 μm), with a mean aspect ratio of 1.3 (standard deviation = 0.1). The ellipsoidal shape is typical of the H-$CoFe_2O_4/SiO_2$ sample because it was not observed on the three blank samples where a more usual spherical shape was obtained (Figure 4b−d).

The magnetic properties of the samples were analyzed by SQUID magnetometry. Figure 5a shows the magnetization−demagnetization curves obtained for the H-$CoFe_2O_4/SiO_2$ and $CoFe_2O_4/SiO_2$ samples. The resulting magnetic parameters of the samples are given in Table 1. The two curves are characteristic of composite materials containing ferrimagnetic nanoparticles with a blocked magnetic moment.[45] In both cases, strong magnetic susceptibility and saturation magnetization (m_s) are observed simultaneously with the presence of a relatively important hysteresis at low field intensity (see the inset in Figure 5a). On the contrary, because of the unblocked magnetic moment of the γ-Fe_2O_3 nanoparticles, the magnetization−demagnetization curves of the two γ-Fe_2O_3-based samples are typical of a superparamagnetic behavior with no hysteresis (see Figure S5 in the Supporting Information for the curves). The values of m_s allowed us to determine the mass

dx.doi.org/10.1021/la501547q | Langmuir 2014, 30, 9190−9200

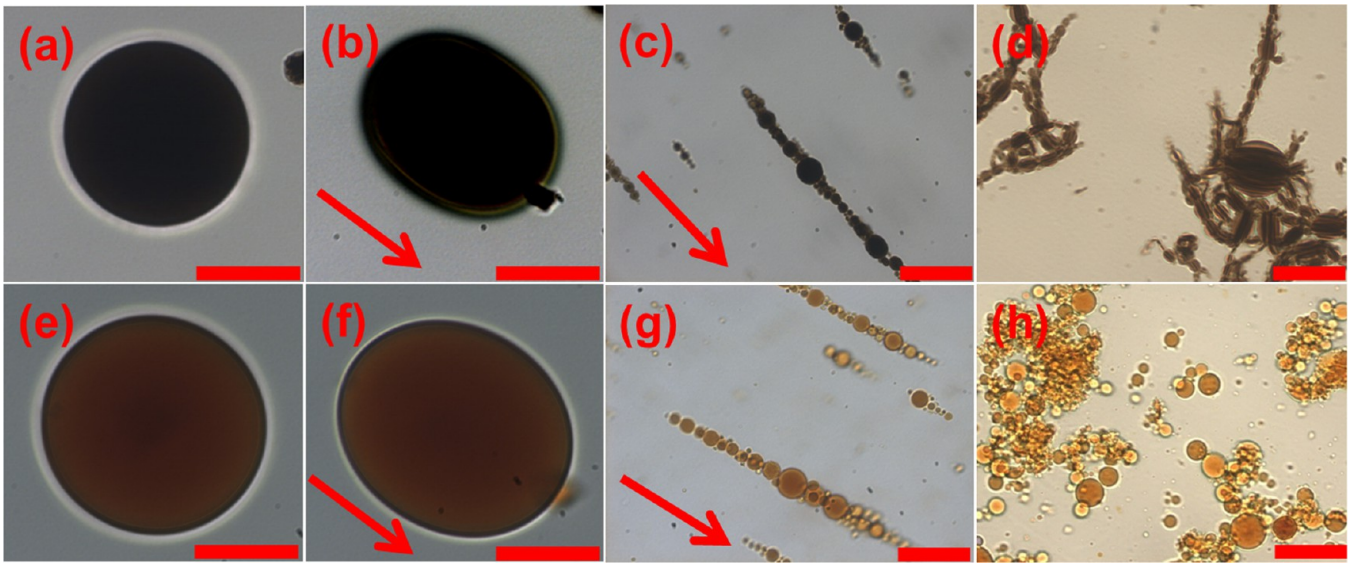

Figure 6. Optical microscopy images showing the influence of an external magnetic field on the water-in-oil droplets. (a) Isolated water-in-oil $CoFe_2O_4/SiO_2$ droplet in the absence of magnetic field. (b) The same droplet in the presence of magnetic field (H = 250 Oe). (c) $CoFe_2O_4/SiO_2$ emulsion preparation in the presence of the magnetic field (H = 250 Oe). (d) $CoFe_2O_4/SiO_2$ emulsion preparation in the absence of the magnetic field, after one night in the presence of the field (H = 1500 Oe). (e) Isolated water-in-oil γ-Fe_2O_3/SiO_2 droplet in the absence of magnetic field. (f) The same droplet in the presence of magnetic field (H = 250 Oe). (g) γ-Fe_2O_3/SiO_2 emulsion preparation in the presence of the magnetic field (H = 250 Oe). (h) γ-Fe_2O_3/SiO_2 emulsion preparation in the absence of the magnetic field, after one night in the presence of the field (H = 1500 Oe). The scale bar is 30 μm. The arrows correspond to the direction of the applied field.

fractions in magnetic nanoparticles, w_{NP}. A high value of w_{NP} was obtained in all of the samples (w_{NP} = 33.7% for the H-$CoFe_2O_4/SiO_2$ microellipsoids). No major effect of the external magnetic field was observed on the magnetization−demagnetization curves of the $CoFe_2O_4$-based samples, because the coercitive fields (H_c) and the remanent magnetizations (M_R) were almost the same (see Table 1). This was first surprising for us: larger values for H_c and M_R would have been expected for the sample synthesized under field, because the external magnetic field strongly increased the structural anisotropy of these materials. However, the disordered packing of the particles in the powdered form may cancel the effect of their intrinsic anisotropy. Nevertheless, the structural difference between the two $CoFe_2O_4$-based samples was confirmed by some of the magnetic measurements. First, the initial magnetization, M_0, which was taken before the application of the magnetic field during the measurements, is non-negligible for the H-$CoFe_2O_4/SiO_2$ sample, to the contrary of the reference samples (see Table 1). The existence of M_0 is thus related to the applied magnetic field during the synthesis of this sample. Furthermore, the two samples can be distinguished by the profile of their ZFC and FC curves, which represent their magnetization versus temperature at low magnetic field (H = 50 Oe), after cooling them in the absence and in the presence of the field, respectively (see Figure 5b). The blocking temperature, T_b, corresponds to the maximum of magnetization in the ZFC curve. When this temperature is reached, the time needed for alignment by Neel rotation of the magnetic moments of the nanoparticles in the direction of the applied magnetic field is becoming shorter than the time used to measure the magnetization of the nanoparticles.[37] Above this temperature, the magnetization decreases because the thermal fluctuations of the magnetic moment increase, and the ZFC and FC curves generally overlap. Here, for the two $CoFe_2O_4$-based samples, T_b is too high to be determined (T_b > 400 K). However, for the H-$CoFe_2O_4/SiO_2$ sample, the smaller value of the magnetization at 400 K in the ZFC and FC curves may indicate a larger value of T_b. This can be interpreted using eq 2, which derives from the well-known Neel−Brown equation.[37,46]

$$25kT_b = KV + E_{dd} \quad (2)$$

Equation 2 shows that T_b depends on KV, the magnetic anisotropy energy, and on E_{dd}, the energy resulting from the magnetic dipolar interactions between the magnetic nanoparticles. KV is related to the nature of the magnetic nanoparticles, and the high value of T_b in the two $CoFe_2O_4$-based samples is therefore explained by the large value of KV. This was confirmed by the ZFC-FC measurements on the γ-Fe_2O_3 based samples where a value of T_b of only 85K was found, due to their smaller value of KV (see Table 1 and Figure S5 in the Supporting Information, for the ZFC-FC curves). Nevertheless, the value of KV being identical in the two $CoFe_2O_4$-based samples, the probable larger value of T_b in the H-$CoFe_2O_4/SiO_2$ sample can only be explained by its larger value of E_{dd}. The larger strength of the magnetic dipolar interactions in this sample is in agreement with the larger aggregation state of the $CoFe_2O_4$ nanoparticles, which are organized in large chains in the silica matrix. It is however important to note that the magnetic dipolar interactions cannot be totally neglected for the $CoFe_2O_4/SiO_2$ sample synthesized at zero field. Indeed, additional ZFC-FC measurements were performed on a sample obtained by dispersing the $CoFe_2O_4$ nanoparticles in a silica gel, at a dilution sufficiently high (w_{NP} = 0.7%) to neglect the magnetic dipolar interactions. In that case, a value of T_b = 390 K was obtained, which is smaller than that for the $CoFe_2O_4/SiO_2$ sample (see Figure S6 in the Supporting Information for the ZFC-FC curve).

Formation Mechanism of the Microellipsoids. The application of an external magnetic field during the synthesis of the H-$CoFe_2O_4/SiO_2$ sample results in two structural features:

dx.doi.org/10.1021/la501547q | Langmuir 2014, 30, 9190−9200

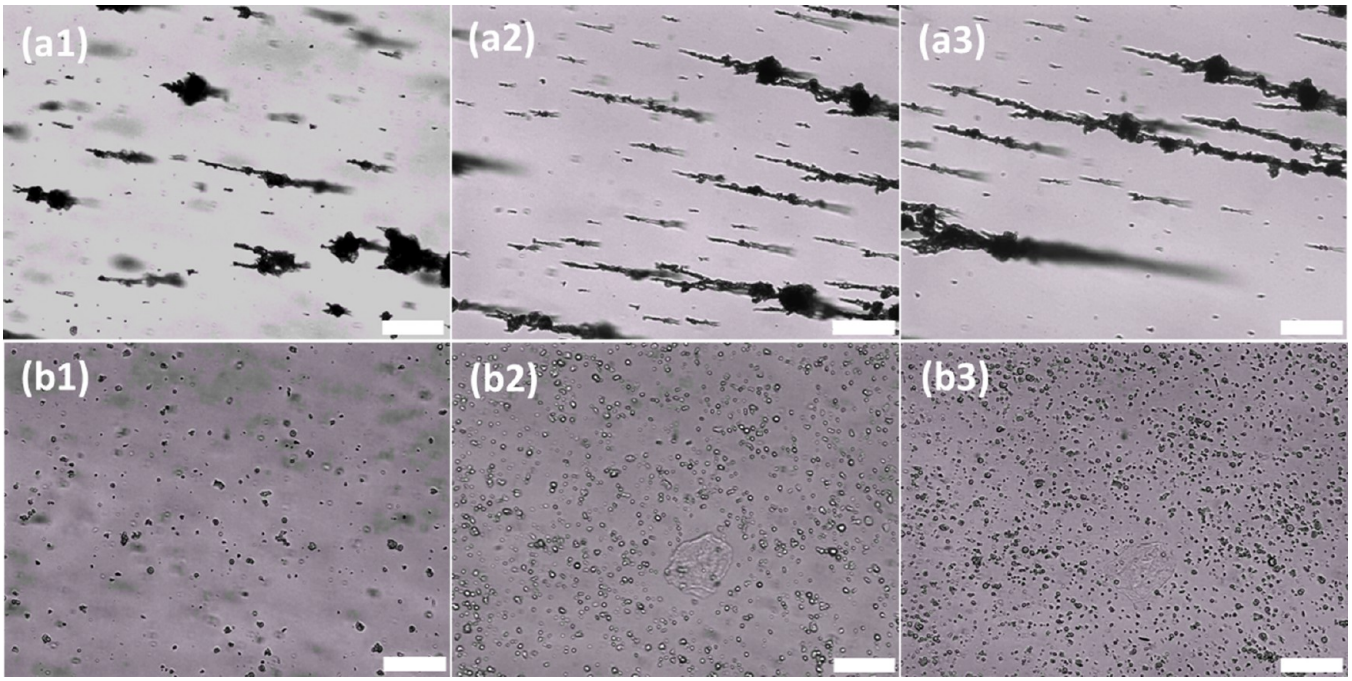

Figure 7. Optical micrographs (magnification ×40) of the aqueous dispersions of the microparticles, at different selected times. (a1−a3) H-$CoFe_2O_4/SiO_2$ microellipsoids at t = 1 s (a1), 2 min (a2), and 5 min (a3). (b1−b3) γ-Fe_2O_3/SiO_2 microspheres at t = 1 s (b1), 2 min (b2), and 5 min (b3). The scale bar is 30 μm.

(i) an internal structure characterized by the chaining of the magnetic nanoparticles; and (ii) an ellipsoidal morphology. As was already mentioned, the field-induced chaining of the magnetic nanoparticles has been well described by many authors, and has been explained by the intensification of the dipolar interactions between the nanoparticles in the presence of the magnetic field. On the contrary, it was more difficult to understand how the shape of the microparticles is influenced by the magnetic field. To clarify this point, the following additional experiences were performed. First, an isolated and large water-in-oil droplet (more than 50 μm in size) containing the $CoFe_2O_4$ nanoparticles and the silica precursor was observed using optical microscopy. When a magnetic field was applied, the droplet was elongated in the direction of the magnetic field, thus acquiring an ellipsoidal shape (Figure 6a,b). Because the experience was performed before gelation of silica, when the magnetic field was cut, the droplet returned to its spherical shape, indicating the reversibility of the elongation phenomenon. In a second experience, the water-in-oil emulsion resulting in $CoFe_2O_4/SiO_2$ samples was submitted to the same magnetic field. In that case, the droplets were also elongated along the direction of the magnetic field. However, the observation was limited because of the small size of the droplets, and because of their alignment in the direction of the field. The chaining of the droplets is due to the existence of induced magnetic moments, resulting in the appearance of magnetic dipolar interactions between the droplets (Figure 6c). When the $CoFe_2O_4$ nanoparticles were replaced by the γ-Fe_2O_3 nanoparticles, the ellipsoidal shape was still detected for a large and isolated water-in-oil droplet, although its aspect ratio was less pronounced (Figure 6e,f). However, the only behavior observed in the emulsion resulting in γ-Fe_2O_3/SiO_2 samples was the alignment of the droplets in the direction of the magnetic field (Figure 6g).

The elongation of droplets under applied magnetic field has already been mentioned in several systems, such as in concentrated aqueous droplets of magnetic nanoparticles resulting from demixed ferrofluids.[47−49] It has been attributed to the effect of the magnetic surface forces appearing along the normal. These forces are stronger on the poles of the magnetized droplets, which therefore tend to be elongated along the external magnetic field.[49] It has been shown that elongation of the magnetic droplets depends on the competition between their magnetic energy and their interfacial energy.[47,48] It has been demonstrated that the magnetic energy is related to the magnetization of the droplet, which increases with the saturation magnetization of the nanoparticles and with their magnetic dipolar interactions. Therefore, for the same concentration of nanoparticles and for the same external magnetic field, the magnetic energy is stronger for the $CoFe_2O_4/SiO_2$ droplets than for the γ-Fe_2O_3/SiO_2 droplets. When the magnetic energy is not sufficient to overcome the interfacial energy, the droplets remain in spherical shape, as it is observed in the γ-Fe_2O_3/SiO_2 emulsion. On the contrary, the ellipsoidal shape of the $CoFe_2O_4/SiO_2$ droplets is favored by their larger magnetic energy.

Finally, we found that the elongation of the $CoFe_2O_4/SiO_2$ aqueous droplets became irreversible after one night under magnetic field, because the ellipsoidal shape of the droplets was maintained in the absence of applied magnetic field (Figure 6d). We believe that the ellipsoidal shape of the $CoFe_2O_4/SiO_2$ sol droplets is "frozen" by the silica gelation after a few hours. The irreversibility of the elongation of the droplets may also be favored by the strong chaining of the $CoFe_2O_4$ nanoparticles inside the droplets along the direction of the main axis of the ellipsoid.

Colloidal Behavior of the Microellipsoids. The colloidal behavior of the H-$CoFe_2O_4/SiO_2$ microellipsoids was determined by following the evolution of their aqueous dispersion

dx.doi.org/10.1021/la501547q | Langmuir 2014, 30, 9190−9200

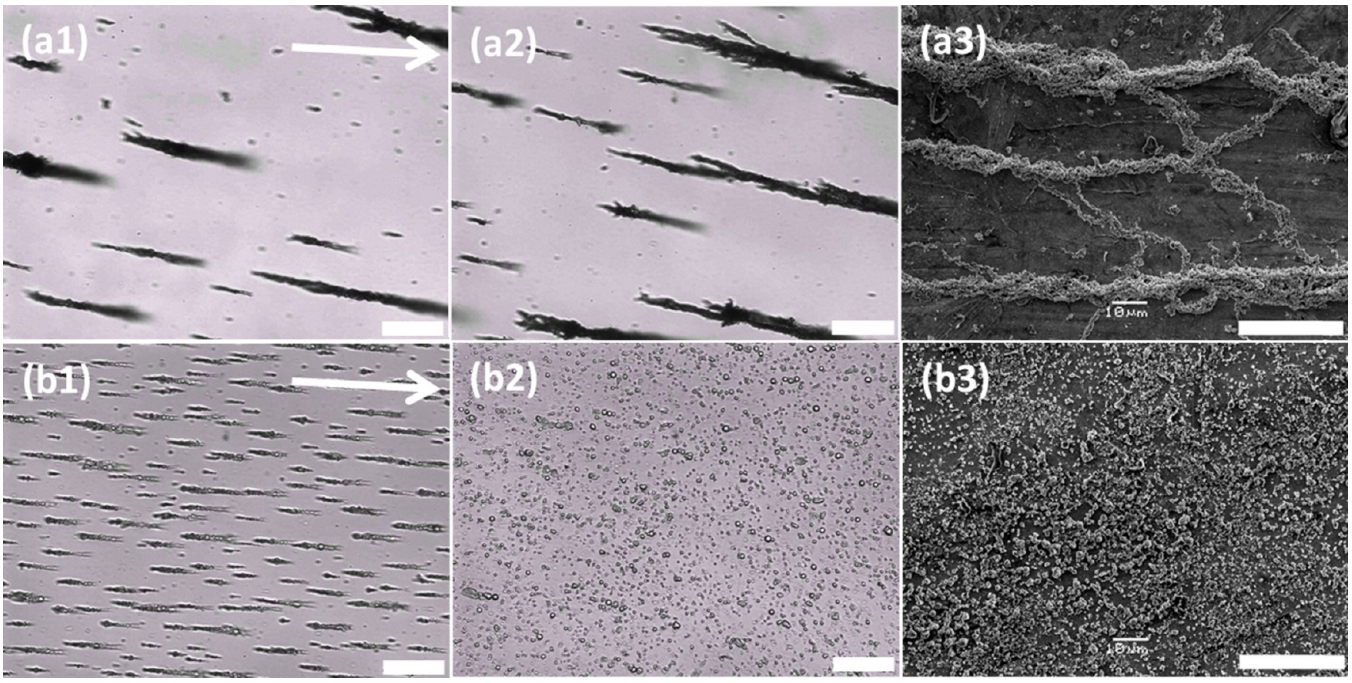

Figure 8. Optical micrographs (magnification ×40) and SEM images of the aqueous dispersions of the microparticles at different selected times, after application of magnetic field during 1 min. (a1−a3) H-$CoFe_2O_4/SiO_2$ microellipsoids. (a1) Optical micrograph at t = 1 s. (a2) Optical micrograph at t = 1 min. (a3) SEM image of the dried dispersion. (b1−b3) γ-Fe_2O_3/SiO_2 microspheres. (b1) Optical micrograph at t = 1 s. (b2) Optical micrograph at t = 1 min. (b3) SEM image of the dried dispersion. The scale bar is 30 μm. The arrows correspond to the direction of the applied field.

with an optical microscope. For comparison, these observations were also performed on the aqueous dispersions of the $CoFe_2O_4/SiO_2$ and γ-Fe_2O_3/SiO_2 samples. After inducing the dispersion of the microparticles by ultrasonic treatment and increase of the pH to 9, two kinds of experiments were made. The first set of experiments was made in the absence of applied magnetic field. Figure 7 shows the resulting optical micrographs at t = 1 s, 2 min, and 5 min, for the H-$CoFe_2O_4/SiO_2$ and γ-Fe_2O_3/SiO_2 dispersions. The microellipsoids were found to be slightly aggregated in small and irregular chains at the beginning of the observation (Figure 7a1). It was impossible to determine if these aggregates resulted from an incomplete dispersion of the particles or from a very fast aggregation in water immediately after the ultrasonic treatment, although TEM and SEM microscopies showed that the particles are not coalesced. Furthermore, we observed a rapid growth of the length and width of these chains (Figure 7a2,a3). A more accurate observation revealed that the lateral and longitudinal growth of the chains results from short-range directional attractive forces between the aggregates (see the complete movie in the Supporting Information). The γ-Fe_2O_3/SiO_2 microspheres exhibited a completely different behavior, because they remained perfectly dispersed during the entire period of observation (Figure 7b1−b3). It should also be noted that the directional aggregation of the particles was observed with a lesser extent for the $CoFe_2O_4/SiO_2$ dispersion (see the movies in the Supporting Information). These differences can be explained in terms of dipolar magnetic interactions existing between the microparticles. The magnetic dipolar interaction between two particles is attractive and maximum when their magnetic moments (μ_T) are in head-to-tail configuration. The energy of the magnetic dipolar interaction between two aligned particles having the same value of μ_T, E_{dd}, is thus expressed by eq 3.[38]

$$E_{dd} = \mu_0 {\mu_T}^2/(2\pi d^3) \quad (3)$$

where μ_0 is the magnetic permeability of vacuum, and d is the distance between the two particles.

Equation 3 shows that the larger is the value of μ_T, the stronger are the dipolar magnetic interactions. Because of the fast Neel motion of the magnetic moments of the γ-Fe_2O_3 nanoparticles, the γ-Fe_2O_3/SiO_2 particles have no net moment (μ_T = 0) and do not present any magnetic dipolar interactions in the absence of external magnetic field. The limited aggregation observed in the $CoFe_2O_4/SiO_2$ dispersion may be due to the existence of small permanent magnetic moments resulting from the addition of the blocked individual magnetic moments of the $CoFe_2O_4$ nanoparticles. For the H-$CoFe_2O_4/SiO_2$ microellipsoids, the value of μ_T could be considerably increased by the anisotropic distribution of the $CoFe_2O_4$ nanoparticles resulting in a large extent of the aggregation. Therefore, the $CoFe_2O_4$-based samples can be considered as colloidal micromagnets, the presence of the magnetic field during their synthesis reinforcing this feature.

The second set of experiments was carried out immediately after submitting the colloidal dispersions to a magnetic field during 1 min (Figure 8). It is well-known that magnetic dipolar interactions are increased by the presence of an external magnetic field.[38] Therefore, we observed a chaining of the particles in the direction of the external magnetic field, whatever the sample. However, the chains formed for the γ-Fe_2O_3/SiO_2 sample were small, and when the magnetic field was stopped, the microspheres were immediately redispersed (Figure 8b1−b3). On the contrary, very large permanent chains (about 1 mm in length and 10 μm in width) were formed for the microellipsoids (Figure 8a1−a3). Interestingly, these colloidal chains were isolated on a surface by simple settlement and evaporation of the water, which allowed their observation by SEM (Figure 8a3). The preparation of permanent chains is

dx.doi.org/10.1021/la501547q | Langmuir 2014, 30, 9190−9200

still a challenge in colloidal chemistry, although several authors already claimed their preparation.[15−25,39−41] Here, permanent fibrous chains are spontaneously formed in water, and their strength and size can be increased by reinforcing the magnetic dipolar interactions with an external magnetic field applied during 1 min.

CONCLUSION

In summary, we have demonstrated that magnetic silica colloids having both an original morphology and an anisotropic organization at the nanoscopic level can be prepared through the synergistic effect of nanoparticles possessing a high magnetic anisotropy, and external magnetic field during the synthesis. While the conventional ESE method usually leads to magnetic silica microspheres with an isotropic distribution of the magnetic nanoparticles,[43,44] we have obtained here magnetic silica microellipsoids containing magnetic nanoparticles aggregated in large chains. At larger scale, these particles exhibit in consequence some strong permanent magnetic moments that are responsible for the existence of magnetic dipolar interactions. Therefore, when they are dispersed in water, the microellipsoids self-assemble into large and irregular chains. These interactions can be reinforced by the use of external magnetic field, allowing the preparation of very large permanent chains. A more systematic study is now underway for a better understanding of the influence of the different parameters (concentration and size of the magnetic nanoparticles, strength of the magnetic field, etc.) on the structure and magnetic properties of these materials. Furthermore, the monodispersity of these particles remains to be improved. This may be reached through a better control of the shearing conditions in the emulsion preparation, or by operating in a microfluidics device. This research illustrates how nanocomposite particles exhibiting complex architectures can be elaborated through simple, fast, and low-cost methods, such as the use of external fields in combination with soft chemistry. Thanks to their unusual properties and the simplicity of their preparation, new fields of application in biomedicine, environment, or optoelectronics might be opened for these materials. Recent studies on the use of nanocomposite particles prepared through the assistance of a magnetic field as biophysical models,[17] adsorbents for water treatment,[22] microstirrers,[23] viscosity sensors,[27] magnetic ink,[30] or as template for the preparation of bulk materials with anisotropic mechanical strength[32,34] are good examples of the potential of this work.

EXPERIMENTAL SECTION

Synthesis. The magnetic $CoFe_2O_4$ nanoparticles were synthesized according to a previously reported method.[42,50] Briefly, stoichiometric aqueous mixtures of cobalt(II) nitrate ($Co(NO_3)_2$) and iron(III) nitrate ($Fe(NO_3)_3$) were prepared with a total concentration of 10^{-1} mol L^{-1}. Sodium hydroxide (NaOH, 10 mol L^{-1}) was added to increase the pH to 13 under vigorous stirring. The mixture was stirred for 1 h at room temperature and then transferred to the Teflon vessel of an autoclave. The autoclave was then introduced to an oven at 200 °C. The oven was heated during an incubation time of 120 h. The precipitate obtained after the temperature of the suspension naturally fell to 25 °C was isolated, and then dispersed in an aqueous solution of hydrochloric acid. The γ-Fe_2O_3 nanoparticles used in this study were synthesized according to a procedure described elsewhere.[51,52] Magnetite (Fe_3O_4) nanoparticles were first prepared by Massart's method.[51] Next, the Fe_3O_4 nanoparticles were oxidized to γ-Fe_2O_3 and dispersed in acid medium by adding HNO_3 and $Fe(NO_3)_3$.[52]

The H-$CoFe_2O_4/SiO_2$ microellipsoids were prepared via a modified ESE (emulsion solvent evaporation) sol−gel method,[43] which has already been published.[44] First, 1 mL of a precursor solution was prepared by adding 0.2 mL of a 0.15 mol L^{-1} HNO_3 aqueous solution to 0.8 mL of tetraethoxysilane (TEOS). This mixture was vigorously stirred for 45 min. During this period, TEOS was hydrolyzed up to an adequate level to obtain a monophasic solution. Next, 2 mL of a magnetic sol with an equivalent concentration of iron [Fe] = 0.8 mol L^{-1} was formed by adding the precursor solution to 1 mL of an aqueous dispersion of $CoFe_2O_4$ nanoparticles. The magnetic sol was stirred during 5 min before being added dropwise to 18 mL of an organic phase composed of a vegetable oil (usually commercial rapeseed oil) containing 0.1% (w/w) of the emulsifier Arlacel P135. The water-in-oil emulsion thus formed was stirred during 30 min and then transferred into a Buchner flask connected to a water aspirator. The ethanol formed by hydrolysis of TEOS was thus evaporated from the dispersed phase during 35 min under reduced pressure (35 mmHg), at a temperature fixed at 35 °C by way of a water bath around the flask. Next, the system was brought back to atmospheric pressure, and the flask containing the emulsion was placed in the center of the area between two cuboid ferrite magnets in parallel and was mechanically stirred for one night. It was checked that for this geometry, the magnetic field was constant (H = 1500 Oe) in the area containing the flask. The emulsion was finally broken by addition of a large amount of acetone. The mixture was stirred during 5 min, and the particles were recovered with a magnet. They were washed several times with acetone and water, and dried in an oven at 70 °C for 4 h. The same procedure was used for the preparation of the $CoFe_2O_4/SiO_2$, γ-Fe_2O_3/SiO_2, and H-γ-Fe_2O_3/SiO_2 reference samples, except that γ-Fe_2O_3 nanoparticles was used instead of $CoFe_2O_4$ nanoparticles, and/or that the emulsion was not placed between the two cuboid ferrite magnets.

Characterization Methods. Transmission electron microscopy (TEM) was made on microtomed samples using a JEM JEOL 100 CX microscope operating at 100 kV. In this aim, the particles were crushed in a mortar, embedded in a resin (AGAR 100) polymerized at 70 °C during 2 days, cut in 70 nm thin sections using a LEICA ULTRACUT UCT microtome apparatus, and deposited on a copper grid. The samples were also observed by scanning electron microscopy (SEM) on a SEM-FEG Hitachi SU-70 apparatus. The images were taken in secondary electron mode with an accelerating voltage of 5 kV. Prior to analysis, the materials were coated with a thin layer of gold by sputter deposition. The size distribution of the particles and their mean aspect ratio were determined from SEM pictures analyzed using the ImageJ software. Magnetic characterizations of the samples were made on a SQUID magnetometer (Quantum Design MPM-5S apparatus). The magnetization−demagnetization curves were taken at 300 K on a given weight of dry material encapsulated in a cell, by measuring the magnetization of the samples for a magnetic field H varying from −50 000 to +50 000 Oe. For the ZFC-FC measurements, the same cells containing the samples were used. The zero field cooled (ZFC) magnetization versus temperature measurements were carried out by cooling the $CoFe_2O_4$ composite samples and the γ-Fe_2O_3 composite samples, respectively, from 300 to 150 K and from 300 to 20 K. A field of 50 Oe then was applied and the magnetizations measured while the $CoFe_2O_4$ and the γ-Fe_2O_3 composite samples were heated respectively from 150 to 400 K and from 20 to 245 K. The field cooled (FC) measurements were performed in the same manner with the difference that the field was applied before cooling. All of the measured magnetizations (m, in emu per g of sample) were normalized to 1 g of magnetic material (M, in emu per g of magnetic nanoparticles) by dividing m by the weight fraction of magnetic nanoparticles, w_{NP}. The values of w_{NP} were obtained by $w_{NP} = m_s/M_s$, where m_s and M_s are the values of magnetization saturations corresponding, respectively, to the composite samples and to the dry pure magnetic nanoparticles. The values of M_s were determined using the magnetization−demagnetization curves of the pure nanoparticles in powdered form (M_s = 62 and 54 emu g^{-1} of magnetic nanoparticles for $CoFe_2O_4$ and γ-Fe_2O_3, respectively).

dx.doi.org/10.1021/la501547q | Langmuir 2014, 30, 9190−9200

The formation of the microellipsoids was studied using an optical microscope (Zeiss) equipped with an objective lens (×40 magnification). Isolated magnetic droplets dispersed in the organic phase (vegetable oil +0.1% of Arlacel P135) were prepared directly on the microscope slides by adding small drops of magnetic sol to the organic phase. The emulsion preparations and the isolated droplets were observed at zero field, and under a magnetic field obtained with a Nd−B−Fe magnet (H = 250 Oe). The colloidal behavior of the aqueous dispersions of the particles was examined using the following procedure. The dry particles (m = 0.01 g) were first dispersed in 1 mL of an aqueous ammonia solution at pH = 9. At this value of pH, the silica surface of the particles is negatively charged, and their dispersion in water is favored by their electrostatic repulsion. Hence, the dispersion was sonicated during 10 min using an ultrasound bath, and was then submitted to settlement during 1 min to eliminate the remaining large aggregates. Finally, a drop of the dispersion was immediately deposited between two microscope slides separated by a spacer, and was observed with the optical microscope (×40 magnification). For a series of experiences, a Nd−B−Fe magnet was applied during 1 min in the proximity of the slides containing the dispersion just before the observation. For the observation of the dried dispersions by SEM microscopy, a drop of the dispersion was deposited on a SEM mount, which was let between two Nd−B−Fe cuboid magnets in parallel during 1 min (H = 1500 Oe). The dispersion was then dried during the night at ambient temperature in the absence of magnetic field.

■ ASSOCIATED CONTENT

Ⓢ Supporting Information

Optical microscopy movies, characterization of the magnetic nanoparticles, photograph of the experimental setup, additional TEM images, elemental mapping by SEM-EDS, and additional magnetic measurements. This material is available free of charge via the Internet at http://pubs.acs.org.

■ AUTHOR INFORMATION

Corresponding Author

*E-mail: sebastien.abramson@upmc.fr

Notes

The authors declare no competing financial interest.

■ ACKNOWLEDGMENTS

We thank Aude Michel, Delphine Talbot, and Anh-Tu Ngo for their technical support, and the internship students Daniel Sittler and Malik Tebbakh. SEM microscopy and EDS analysis in the IMPC (FR 2482) was supported by the C'Nano projects of the Region Ile-de-France.

■ REFERENCES

(1) Matijević, E. Preparation and Properties of Uniform Size Colloids. *Chem. Mater.* **1993**, *5*, 412−426.

(2) Matijević, E. Uniform Inorganic Colloids Dispersions. Achievements and Challenges. *Langmuir* **1994**, *10*, 8−16.

(3) Xia, Y.; Gates, B.; Yin, Y.; Lu, Y. Monodispersed Colloidal Spheres: Old Materials with New Applications. *Adv. Mater.* **2000**, *12*, 693−713.

(4) Lu, Y.; Yin, Y.; Xia, Y. Three-Dimensional Photonic Crystals with Non-spherical Colloids as Building Blocks. *Adv. Mater.* **2001**, *13*, 415−420.

(5) Perro, A.; Reculusa, S.; Ravaine, S.; Bourgeat-Lami, E.; Duguet, E. Design and Synthesis of Janus Micro- and Nanoparticles. *J. Mater. Chem.* **2005**, *15*, 3745−3760.

(6) Cortie, M. B.; Mc Donagh, A. M. Synthesis and Optical Properties of Hybrid and Alloy Plasmonic Nanoparticles. *Chem. Rev.* **2011**, *111*, 3713−3735.

(7) Li, F.; Josephson, D. P.; Stein, A. Colloidal Assembly: The Road from Particles to Colloidal Molecules and Crystals. *Angew. Chem., Int. Ed.* **2011**, *50*, 360−388.

(8) Lu, A.-H.; Salabas, E. L.; Schüth, F. Magnetic Nanoparticles: Synthesis, Protection, Functionalization, and Application. *Angew. Chem., Int. Ed.* **2007**, *46*, 1222−1244.

(9) Jeong, U.; Teng, X.; Wang, Y.; Yang, H.; Xia, Y. Superparamagnetic Colloids: Controlled Synthesis and Niche Applications. *Adv. Mater.* **2007**, *19*, 33−60.

(10) Liu, J.; Qiao, S. Z.; Hu, Q. H.; Lu, G. Q. M. Magnetic Nanocomposites with Mesoporous Structures: Synthesis and Applications. *Small* **2011**, *7*, 425−443.

(11) Zhou, L.; Yuan, J.; Wei, Y. Core-Shell Structural Iron Oxide Hybrid Nanoparticles: From Controlled Synthesis to Biomedical Applications. *J. Mater. Chem.* **2011**, *21*, 2823−2840.

(12) Behrens, S. Preparation of Functional Magnetic Nanocomposites and Hybrid Materials: Recent Progress and Future Directions. *Nanoscale* **2011**, *3*, 877−892.

(13) Lu, F.; Popa, A.; Zhou, S.; Zhu, J.-J.; Samia, A. C. S. Iron oxide-Loaded Mesoporous Silica Nanocapsules for Controlled Drug Release and Hypertermia. *Chem. Commun.* **2013**, *49*, 11436−11438.

(14) Fontaíña-Troitiño, N.; Liébana-Viñas, S.; Rodríguez-González, B.; Li, Z.-A.; Spasova, M.; Farle, M.; Salgueiriño, V. Room-Temperature Ferromagnetism in Antiferromagnetic Cobalt Oxide Nanooctahedra. *Nano Lett.* **2014**, *14*, 640−647.

(15) Furst, E. M.; Suzuki, C.; Fermigier, M.; Gast, A. P. Permanently Linked Monodisperse Paramagnetic Chains. *Langmuir* **1998**, *14*, 7334−7336.

(16) Goubault, C.; Leal-Calderon, F.; Viovy, J.-L.; Bibette, J. Self-Assembled Magnetic Nanowires Made Irreversible by Polymer Bridging. *Langmuir* **2005**, *21*, 3725−3729.

(17) Koenig, A.; Hébraud, P.; Gosse, C.; Dreyfus, R.; Baudry, J.; Bertrand, E.; Bibette, J. Magnetic Force Probe for Nanoscale Biomolecules. *Phys. Rev. Lett.* **2005**, *95*, 128301(1)−128301(4).

(18) Korth, B. D.; Keng, P.; Shim, I.; Bowles, S. E.; Tang, C.; Kowaleski, T.; Nebesny, K. W.; Pyun, J. Polymer-Coated Ferromagnetic Colloids from Well-Defined Macromolecular Surfactants and Assembly into Nanoparticles Chains. *J. Am. Chem. Soc.* **2006**, *128*, 6562−6563.

(19) Singh, H.; Laibinis, P. E.; Hatton, T. A. Rigid, Superparamagnetic Chains of Permanently Linked Beads Coated with Magnetic Nanoparticles. Synthesis and Rotational Dynamics under Applied Magnetic Fields. *Langmuir* **2005**, *21*, 11500−11509.

(20) Amali, A. J.; Saravanan, P.; Rana, R. K. Tailored Anisotropic Magnetic Chain Structures Hierarchically Assembled from Magneto-responsive and Fluorescent Components. *Angew. Chem., Int. Ed.* **2011**, *50*, 1318−1321.

(21) Ma, M.; Zhang, Q.; Dou, J.; Zhang, H.; Yin, D.; Geng, W.; Zhou, Y. Fabrication of One-Dimensional Fe_3O_4/P(GMA-DVB) Nanochains by Magnetic-Field-Induced Precipitation Polymerization. *J. Colloid Interface Sci.* **2012**, *374*, 339−344.

(22) Gao, M.-R.; Zhang, S.-R.; Jiang, J.; Zheng, Y.-R.; Tao, D.-Q.; Yu, S.-H. One-Pot Synthesis of Hierarchical Magnetite Nanochain Assemblies with Complex Building Units and their Application for Water Treatment. *J. Mater. Chem.* **2011**, *21*, 16888−16892.

(23) Chong, W. H.; Chin, L. K.; Tan, R. L. S.; Wang, H.; Liu, A. Q.; Chen, H. Stirring in Suspension: Nanometer-Sized Magnetic Stir Bars. *Angew. Chem., Int. Ed.* **2013**, *52*, 8570−8573.

(24) Xiong, Y.; Chen, Q.; Tao, N.; Ye, J.; Tang, Y.; Feng, J.; Gu, X. The Formation of Legume-Like Structures of Co Nanoparticles through a Polymer-Assisted Magnetic-Field-Induced Assembly. *Nanotechnology* **2007**, *18*, 345301(1)−345301(5).

(25) Bannwarth, M. K.; Kazer, S. W.; Ulrich, S.; Glasser, G.; Crespy, D.; Landfester, K. Well-Defined Nanofibers with Tunable Morphology from Spherical Colloidal Building Blocks. *Angew. Chem., Int. Ed.* **2013**, *52*, 10107−10111.

(26) Fresnais, J.; Berret, J.-F.; Frka-Petesic, B.; Sandre, O.; Perzynski, R. Electrostatic Co-Assembly of Iron Oxide Nanoparticles and

Polymers: Towards the Generation of Highly Persistent Superparamagnetic Nanorods. *Adv. Mater.* **2008**, *20*, 3877−3881.
(27) Allione, M.; Torre, B.; Casu, A.; Falqui, A.; Piacenza, P.; Di Corato, R.; Pellegrino, T.; Diaspro, A. Rod-Shaped Nanostructures Based on Superparamagnetic Nanocrystals as Viscosity Sensors in Liquid. *J. Appl. Phys.* **2011**, *110*, 064907(1)−064907(6).
(28) Benkoski, J. J.; Breidenich, J. L.; Uy, O. M.; Hayes, A. T.; Deacon, R. M.; Land, H. B.; Spicer, J. M.; Keng, P. Y.; Pyun, J. Dipolar Organization and Magnetic Actuation of Flagella-like Nanoparticle Assemblies. *J. Mater. Chem.* **2011**, *21*, 7314−7325.
(29) Ge, J.; Lee, H.; He, L.; Kim, J.; Lu, Z.; Kim, H.; Goebl, J.; Kwon, S.; Yin, Y. Magnetochromatic Microspheres: Rotating Photonic Crystals. *J. Am. Chem. Soc.* **2009**, *131*, 15687−15694.
(30) Kim, J.; Song, Y.; He, L.; Kim, H.; Lee, H.; Park, W.; Yin, Y.; Kwon, S. Real-Time Optofluidic Synthesis of Magnetochromatic Microspheres for Reversible Structural Color Patterning. *Small* **2011**, *7*, 1163−1168.
(31) Benkoski, J. J.; Bowles, S. E.; Korth, B. D.; Jones, R. L.; Douglas, J. F.; Karim, A.; Pyun, J. Field Induced Formation of Mesoscopic Polymer Chains from Functional Ferromagnetic Colloids. *J. Am. Chem. Soc.* **2007**, *129*, 6291−6297.
(32) Robbes, A. S.; Cousin, F.; Meneau, F.; Dalmas, F.; Boué, F.; Jestin, J. Nanocomposite Materials with Controlled Anisotropic Reinforcement Trigerred by Magnetic Self-Assembly. *Macromolecules* **2011**, *44*, 8858−8865.
(33) Furlan, M.; Brand, B.; Lattuada, M. Magnetic Gelation: A New Method for the Preparation of Polymeric Anisotropic Porous Materials. *Soft Matter* **2010**, *6*, 5636−5644.
(34) Furlan, M.; Lattuada, M. Fabrication of Anisotropic Porous Silica Monoliths by Means of Magnetically Controlled Phase Separation in Sol-Gel Processes. *Langmuir* **2012**, *28*, 12655−12662.
(35) Güell, O.; Sagués, F.; Tierno, P. Magnetically Driven Janus Micro-Ellipsoids Realized via Asymmetric Gathering of the Magnetic Charge. *Adv. Mater.* **2011**, *23*, 3674−3679.
(36) Ghosh, S.; Puri, I. K. Soft Polymer Magnetic Nanocomposites: Microstructure Patterning by Magnetophoretic Transport and Self-Assembly. *Soft Matter* **2013**, *9*, 2024−2029.
(37) Sorensen, C. M. Magnetism. In *Nanoscale Materials in Chemistry*; Klabunde, K. J., Ed.; Wiley-Interscience Publication: New York, 2001; Chapter 6, pp 169−221.
(38) Klokkenburg, M.; Erné, B. H.; Meeldijk, J. D.; Wiedenmann, A.; Petukhov, A. V.; Dullens, R. P. A.; Philipse, A. P. In-Situ Imaging of Field-Induced Hexagonal Columns in Magnetic Ferrofluids. *Phys. Rev. Lett.* **2006**, *97*, 185702(1)−185702(4).
(39) Cataldo, S.; Pignataro, B.; Ruggirello, A.; Bongiorno, C.; Liveri, V. T. The Zero Field Self-Organization of Cobalt/Surfactant Nanocomposite Thin Films. *Nanotechnology* **2009**, *20*, 225605(1)−225605(9).
(40) Salgueiriño-Maceira, V.; Correa-Duarte, M. A.; Huchts, A.; Farle, M. One-Dimensional Assemblies of Silica-Coated Cobalt Nanoparticles: Magnetic Pearl Necklaces. *J. Magn. Magn. Mater.* **2006**, *303*, 163−166.
(41) Guardia, P.; Pérez, N.; Labarta, A.; Battle, X. Controlled Synthesis of Iron Oxide Nanoparticles over a Wide Size Range. *Langmuir* **2010**, *26*, 5843−5847.
(42) Cabuil, V.; Dupuis, V.; Talbot, D.; Neveu, S. Ionic Magnetic Fluid Based on Cobalt Ferrite Nanoparticles: Influence of Hydrothermal Treatment on the Nanoparticle Size. *J. Magn. Magn. Mater.* **2011**, *323*, 1238−1241.
(43) Andersson, N.; Corkery, R. W.; Alberius, P. C. A. One-Pot Synthesis of Well Ordered Mesoporous Magnetic Carriers. *J. Mater. Chem.* **2007**, *17*, 2700−2705.
(44) Abramson, S.; Safraou, W.; Malezieux, B.; Dupuis, V.; Borensztajn, S.; Briot, E.; Bée, A. An Eco-Friendly Route to Magnetic Silica Microspheres and Nanospheres. *J. Colloid Interface Sci.* **2011**, *364*, 324−332.
(45) Claesson, E. M.; Erné, B. H.; Bakelaar, I. A.; Kuipers, B. W. M.; Philipse, A. P. Measurement of the Zero-Field Magnetic Dipole Moment of Magnetizable Colloidal Silica Spheres. *J. Phys.: Condens. Matter* **2007**, *19*, 036105(1)−036105(16).
(46) Brown, W. F. Thermal Fluctuations of a Single-Domain Particle. *Phys. Rev.* **1963**, *130*, 1677−1686.
(47) Bacri, J.-C.; Salin, D.; Massart, R. Study of the Deformation of Ferrofluid Droplets in a Magnetic Field. *J. Phys., Lett.* **1982**, *43*, L179−L184.
(48) Bacri, J.-C.; Salin, D. Bistability of Ferrofluid Drops under Magnetic Field. *J. Magn. Magn. Mater.* **1983**, *39*, 48−50.
(49) Dubois, E.; Perzynski, R.; Boué, F.; Cabuil, V. Liquid-Gas Transitions in Charged Colloidal Dispersions: Small-Angle Neutron Scattering Coupled with Phase Diagrams of Magnetic Fluids. *Langmuir* **2000**, *16*, 5617−5625.
(50) Tourinho, F. A.; Franck, R.; Massart, R.; Perzynski, R. Synthesis and Magnetic Properties of Manganese and Cobalt Ferrite Ferrofluids. *Prog. Colloid Polym. Sci.* **1989**, *79*, 128−134.
(51) Massart, R. Preparation of Aqueous Magnetic Liquids in Alkaline and Acidic Media. *IEEE Trans. Magn.* **1981**, *MAG-17*, 1247−1248.
(52) Cabuil, V. Ferrofluides à base de maghémite: synthèse, propriétés physicochimiques et magnéto-optiques. Ph.D. Thesis, University Pierre et Marie Curie, defended in May 1987.